

## 4.1 Introduction

Since the 1970s, various types of ceramic, glass and glass–ceramic materials have been proposed and used to replace damaged bone in many clinical applications. Hydroxyapatite (HA) has been successfully employed for its excellent biocompatibility. On the other hand, the bioactivity of HA and its reactivity with bone can be improved by the addition of appropriate amounts of  $\text{TiO}_2$  and bioactive glasses, thus obtaining BG-HA- $\text{TiO}_2$  based biocomposites. The loss of an organ or tissue due to cancer, disease or trauma is a critical problem in human health care. A challenging promising approach to address such issue is to create biological or hybrid replacement for implantation into the body. The self-healing potential of the body itself is proposed in the framework of the emerging tissue engineering [R.M. Nerem et al. 1991; L.G. Griffith et al. 2002; R. Lanza et al. 2007; R. Langer et al. 1993].

Hydroxyapatite (HA,  $\text{Ca}_{10}(\text{PO}_4)_6(\text{OH})_2$ ) can form strong chemical bonds with natural bone because of its similar chemical and crystallographic structure like the apatite of living bone. But one of its primary restrictions in clinical use is load-bearing implants because it has poor mechanical property (C. Q. Ning et al. 2000 and K. DE Groot et al. 1980). Our study with the  $\text{SiO}_2\text{-CaO-P}_2\text{O}_5\text{-K}_2\text{O-Al}_2\text{O}_3$  based bioactive glasses suggests that the material could be used in bone replacement for clinical cases. The bioactive glasses have demonstrated the high degree of tolerance for the RBC and WBC which strongly supports its suitability as an alternative for bone replacement (Himanshu Tripathi et al. 2015). Hydroxyapatite ( $\text{Ca}_{10}(\text{PO}_4)_6(\text{OH})_2$ , HA) has been attracting much attention as a material for artificial bones (Hench LL et al. 1998) and scaffolds for tissue engineering.

Artificial implants, such as the total hip replacement, are successful for a limited time, but all orthopedic implants lack three of the most critical characteristics of living tissues: (a) the ability to self-repair; (b) the ability to maintain a blood supply; (c) the ability to modify their structure and properties in response to environmental factors such as mechanical load. A recent study showed that 24% of Charnley hip operations required revision surgery [D.J. Berry et al. 2002]. It is well known that the incorporation of a ceramic reinforcement, e.g. (fibers, whiskers, platelets or particles) in a ceramic matrix improves the mechanical properties.

A good combination of the bioactivity of hydroxyapatite and the favorable mechanical properties of metals are considered as a promising approach to fabricating more perfect biomedical materials for loadbearing applications. There are two creative ways to meet the above idea [L.L. Hench et al. 1998]. One is to make a microcomposite using metal fibers or particles to reinforce the hydroxyapatite [P Ducheyne et al. 1982; De With G et al. 1989; X Zhang et al. 1997]. As natural bones and teeth are composites of hydroxyapatite and collagen. Another way is to fabricate a macrocomposite material using the hydroxyapatite as a coating material on the surface of biomedical metals. Titanium and its alloys coated with plasma sprayed hydroxyapatite which has been widely used in clinical belong to this class of material [K De Groot et al. 1987; Ji H et al. 1992; Y Fu et al. 1998; R McPherson et al. 1995]. But vast differences in physical and thermal properties between the titanium and the hydroxyapatite inevitably limit the use of this kind of material.

## **4.2 Material and Methods**

### **4.2.1 Preparation of Bioglass**

Bioglass (45S5) with the chemical compositions as given in Table 2.1, were prepared from reagent grade chemicals. It was weighted, mixed and melted in 100 ml platinum crucible at  $1400 \pm 5^\circ\text{C}$  with air as furnace atmosphere for 4 hours. Melted glass was poured in water to prepare frit and it was milled to a powder form in a porcelain ball mill for 24 h.

#### **4.2.2 Production of HA**

In the present study, calcium nitrate tetrahydrate ( $\text{Ca}(\text{NO}_3)_2 \cdot 4\text{H}_2\text{O}$ ) (CNT) ( G.S. Chemical Testing Lab. & allied industries, India), phosphoric acid ( $\text{H}_3\text{PO}_4$ ) (Loba Chemie Pvt. Ltd, India) and ammonia ( $\text{NH}_3$ ) (Loba Chemie Pvt. Ltd, India)) were used as initial precursors. The schematic presentation of the procedure [E.M.A. Khalil et al. 2010] is listed in Fig.2.3.

#### **4.2.3 Preparation of BG/HA/ $\text{TiO}_2$ composites**

The HA,  $\text{TiO}_2$  powder were mixed each in weight ratios 5,10,15,20% with bioglass (45S5) powder and compacted at 1500 MPa pressure into cylindrical samples (1 cm, 1 cm) which was sintered at  $1150^\circ\text{C}$  to prepare the composites as shown in Table 4.1.

Table 4.1: Composition of bio-composite (BGHATi1, BGHATi2, BGHATi3, BGHATi4).

Bio-composite Samples	Composition (wt %)		
	BG (45S5)	HA	TiO <sub>2</sub>
BGHATi1	90	05	05
BGHATi2	80	10	10
BGHATi3	70	15	15
BGHATi4	60	20	20

### 4.3 Results and Discussion

#### 4.3.1 Differential Thermal Analysis (DTA)

The DTA traces of biocomposites show that the incorporation of HA and TiO<sub>2</sub> in the base bioactive glass (45S5) causes a decrease in its endothermic peak temperature as well as its exothermic peak temperature. In the differential thermal analysis (DTA) traces of bioactive glasses (Fig.4.1), endothermic peak shows the nucleation region and the exothermic peak corresponding to the crystallization process. Previous studies (E.M.A. Khalil et al.,2010) have shown that in silicate glasses, the presence of transition metal ion's of low doping percentage is not expected to form separate structural units.

TGA curve of biocomposites precursor after drying at 200-900°C for four hour. Three main stages of TGA curve of TiO<sub>2</sub> sample according to the heat profile were observed. The temperature increases from 200 to 240°C as the first stage. The range of temperature 250 to 260°C is attributed to the decomposition of the organic compounds which shows about 8.0 % weight lost (J. Wang et al.2008). The amorphous precursor

was converted to anatase phase as the temperature increases from 270 to 280°C. The TiO<sub>2</sub> anatase was transferred to rutile phase between 720 to 740°C (X. Sun et al.2010).

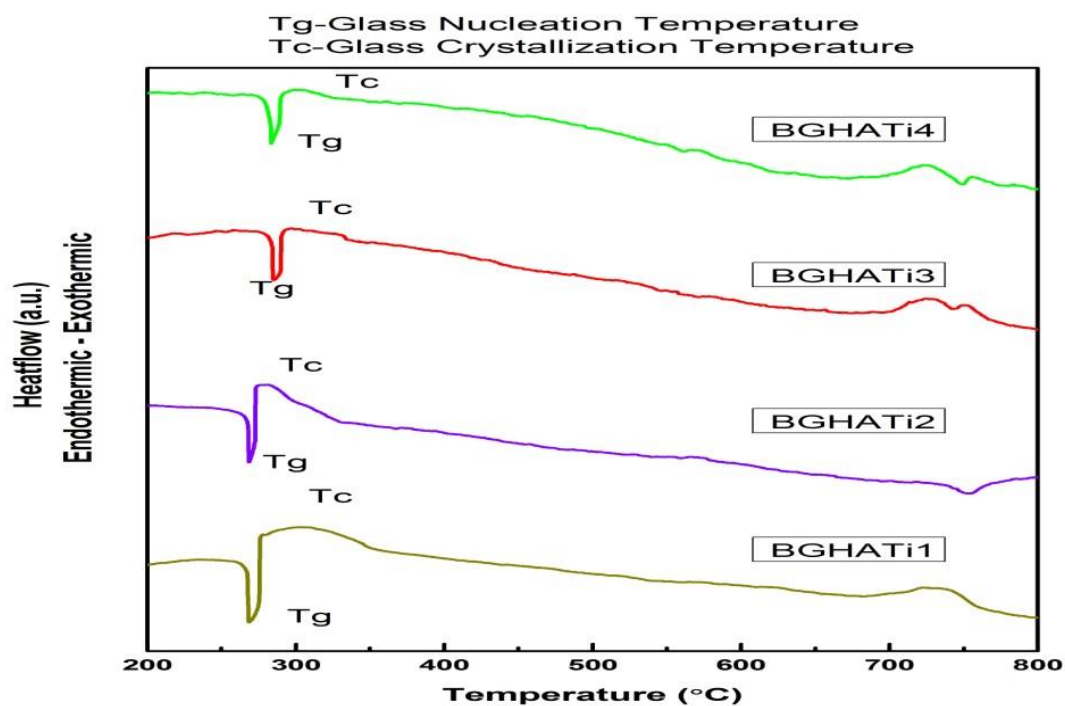


Figure 4.1 DTA/TGA traces of biocomposite.

#### 4.3.2 X-Ray Diffraction (XRD) patterns of biocomposite

The prepared samples of composites are BGHATi1, BGHATi2, BGHATi3, BGHATi4 were characterized by XRD. X-ray powder diffraction data of the prepared biocomposites are shown in Fig. 4.2. The patterns of BGHATi1 composite having high % of BG content do not show any peaks for BG due to its amorphous nature and because the intensity of titania peaks is very weak denoting lower content of titania in the BGHATi1 composite. These peaks are recorded at  $d$  (Å) = 3.24, 2.99, 2.61 forming calcium titanium silicate [CaTi(SiO<sub>5</sub>)] compound (Card No.: 73-2066) and proving interaction between TiO<sub>2</sub> and BG powders. Fig. 4.2 shows the increase of the intensity of calcium titanium silicate oxide peaks denoting more reaction found between the BG

and  $\text{TiO}_2$  [C.C. Wang et al. 1999] as well as the appearance of some peaks of titania (rutile form) at  $d$  ( $\text{Å}$ ) = 2.49, 2.18, 2.06, 1.68 and 1.62 (Card No.: 04-0551) as a result of the conversion of anatase to rutile form that are not reacted with BG powder. In this domain, anatase transforms into rutile format any temperature between 600 and 1000°C [H.M. Kim et al. 1996]. For BGHATi3 composite, Fig. 4.2 shows the increase of intensity of  $\text{CaTi}(\text{SiO}_5)/\text{TiO}_2$  peak at  $d$  ( $\text{Å}$ ) = 3.25 with the disappearance of the peaks at  $d$  ( $\text{Å}$ ) = 2.99. The peaks of rutile increases and became almost four times compared to those of BGHATi4 composite as a result of the highest titania content in the BG/titania composite proving the presence of part of titania powder which does not react with BG powder and converts entirely to the rutile form. These results show possible reactions during transformation at the temperature from 1000 to 1200°C as follows [B.N. Çetiner et al. 2014].

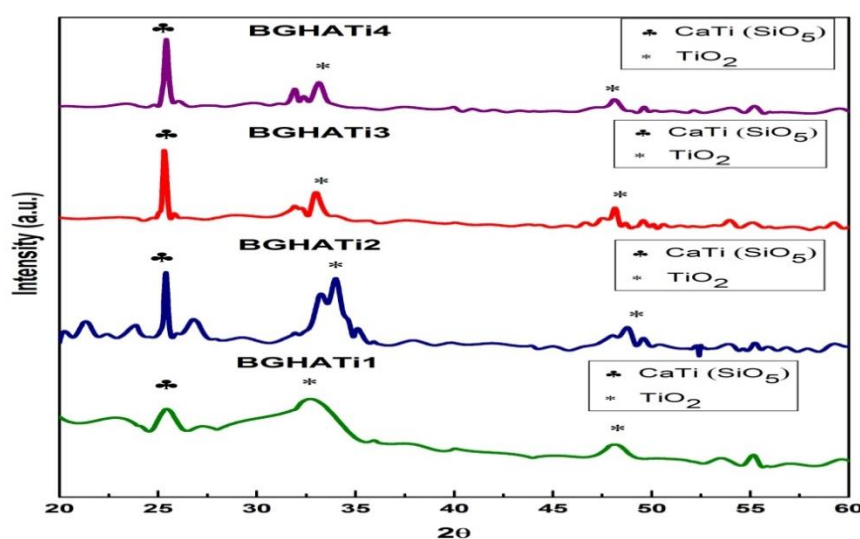
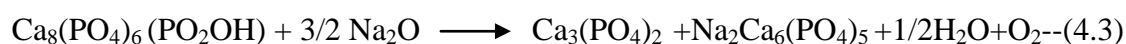


Figure 4.2 X-ray diffraction of the prepared BG/HA/ $\text{TiO}_2$  composites.

### 4.3.3 FTIR assessment

Fig. 4.3 shows the FTIR spectra of titania (TiO<sub>2</sub>), bioactive glass, hydroxyapatite (HA), and their biocomposites (BGHATi1, BGHATi2, BGHATi3, and BGHATi4). The FTIR spectra of BGHATi1 composite having high % of BG showed the typical bands for BG structure with broadening in their bands. The band at 1090 cm<sup>-1</sup> corresponds to the Si–O–Si asymmetric stretching mode, the band at 792 cm<sup>-1</sup> is associated with a Si–O–Si symmetric stretching and the band at 476 cm<sup>-1</sup> is assigned to the Si–O–Si symmetric bending mode and the shoulder at 950 cm<sup>-1</sup> is related to the Si–O–Ca [M.M. Perira et al. 1994]. FTIR spectrum of BGHATi1 composite showed that the bands at 596 and 603 cm<sup>-1</sup> are associated with the stretching vibration of phosphate groups [J.C. Elliott et al. 1994]. The spectra of BGHATi2 and BGHATi3 composites have same behavior like BGHATi1 with broadening in the bands with some shift compared to original BG, HA, titania. The intensity of Ti–O–Ti/Si–O–Si and PO<sub>4</sub><sup>3-</sup> bands increased gradually as a result of the increase of titania content proving interaction between BG, HA, and titania forming CaTi(SiO<sub>5</sub>) compound as in BGHATi4 composite containing the highest material of titania. Fig. 4.3 after soaking in SBF for different time periods is a part of hydroxyapatite in the composition of a prepared composite. It was expected to find the hydroxyl group peaks on 3570 cm<sup>-1</sup>.

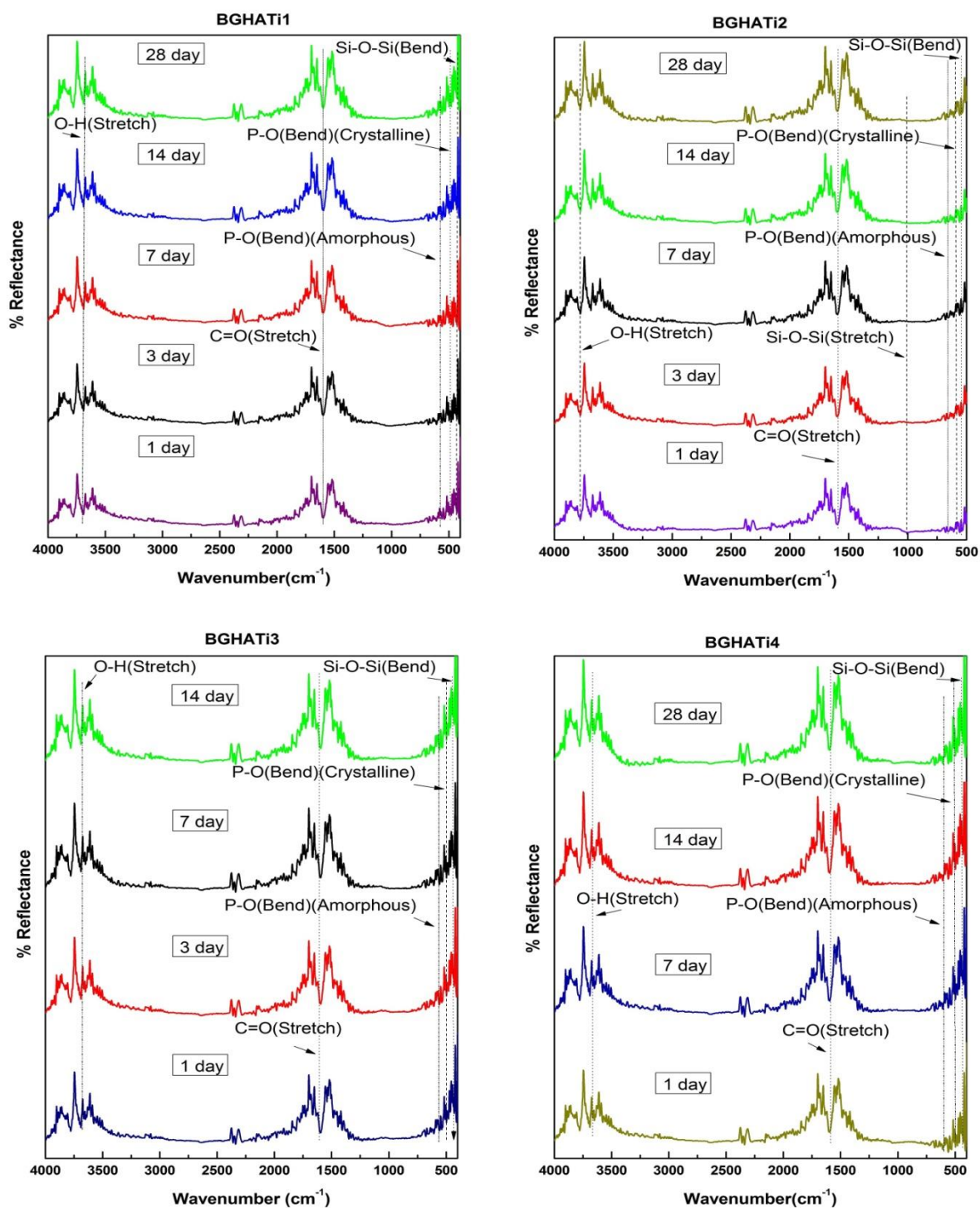


Figure 4.3 The FTIR of BGHATi1, BGHATi2, BGHATi3 and BGHATi4 composite post immersion in SBF after 1,3,7,14,28 days.



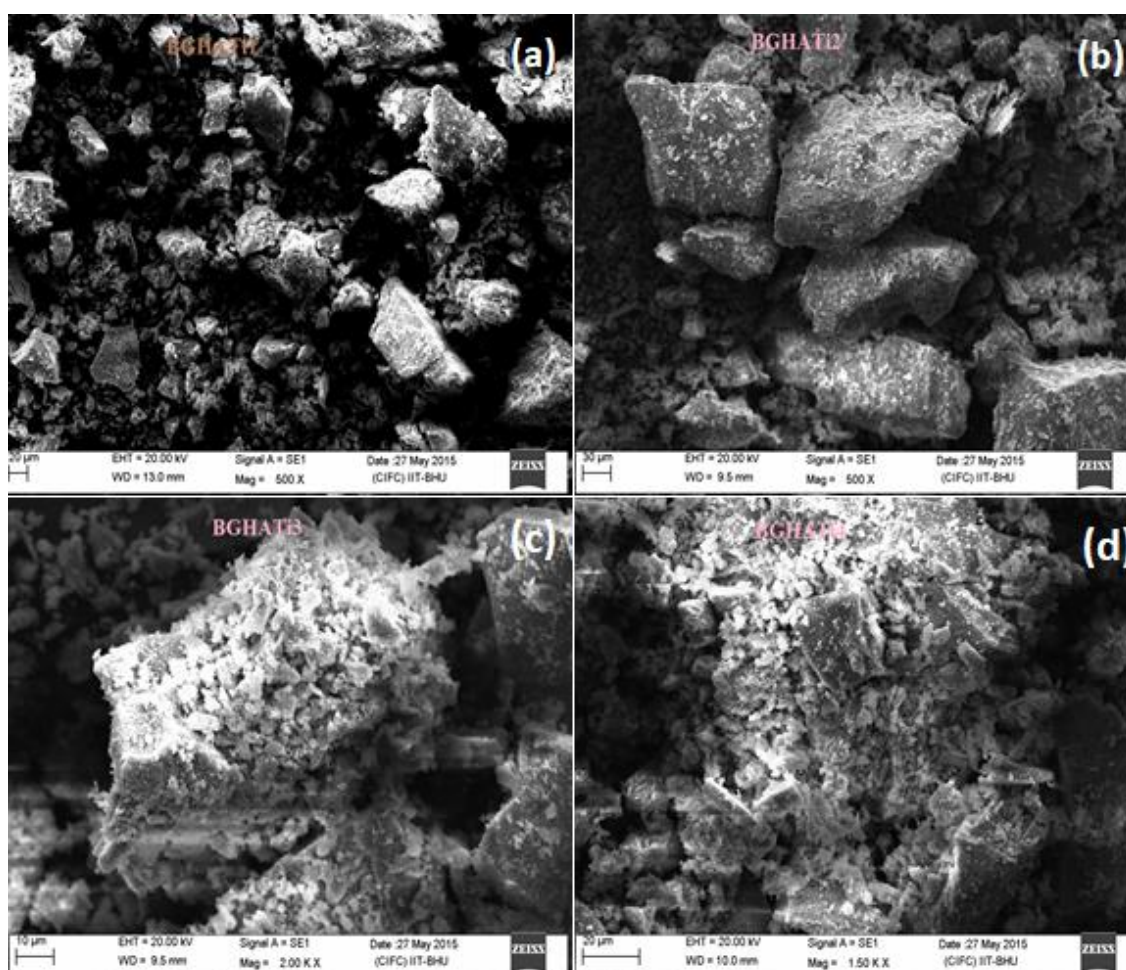
#### 4.3.4 Surface morphology of biocomposite

Post-immersion in SBF the glass releases  $\text{Ca}^{2+}$  and  $\text{Na}^+$  ions from its surface via an exchange with the  $\text{H}_3\text{O}^+$  ion in the SBF to form Si–OH or Ti–OH groups on their surfaces (A.J. Salinas et al. 2002). Water molecules in the SBF simultaneously react with the Si–O–Si or Ti–O–Ti bond to form additional Si–OH or Ti–OH groups. The formed Si–OH and Ti–OH groups induce apatite nucleation, and the released  $\text{Ca}^{2+}$  and  $\text{Na}^+$  ions accelerate apatite nucleation by increasing the ionic activity product of apatite in the fluid (P.N. De Aza et al.2004). As a result, the apatite layer forms onto the composite surface after soaking in SBF in a short period (3days) and this phenomenon is confirmed by SEM of BGHATi composites post-immersion as shown in Fig.4.4(a-d). BGHATi1 biocomposites, shows that this composite has many particles on its surface proving slight formation of apatite layer due to the composite contains high content of silica characterizing melted and dense structure that reduced nucleation of apatite layer compared to other composites. In this domain, the simultaneous dissolution of silicates results in the formation of silanol groups on material's surface, which are essential for nucleation sites resulting in HA formation (C. Sarmento et al.,2004). Once the apatite nuclei formed, they can grow spontaneously by consuming the calcium phosphate ions in the surrounding fluid (P.N. De Aza et al.2000).

For BGHATi2, BGHATi3 and BGHATi4 composites, SEM at the same magnification indicate the presence of rich spherical shapes build upon each other to form a bone-like apatite layer for both composites especially BGHATi4 composites. This result is due to BGHATi4 composites contains the high content of titania which leads to increase of Ti–OH groups at the expense of Si–OH groups resulting in high nucleation of apatite (Fig. 4.4d). In this study, it was observed that the rutile form of titania is the primary phase in

four composites and is essential for improvement of apatite nucleation especially BGHATi3 and BGHATi4 composites compared to BGHATi1 composites containing the low content of titania. The catalytic effect of the Si–OH groups, Ti–OH groups for the apatite nucleation has proven by the observation that silica and titanium will form apatite on their surfaces in SBF are abundant on the composite surfaces (C. Sarmiento et al.,2004; P.N. De Aza et al.,2000 and P.N. De Aza et al.,1999).

EDAX point analyses show that Ca, P and Ti coexist in different properties of the sintered pellet as shown in Fig. 4.4 (e-h) confirming the interfusion between HA and TiO<sub>2</sub> particles before their impinging into the substrate.



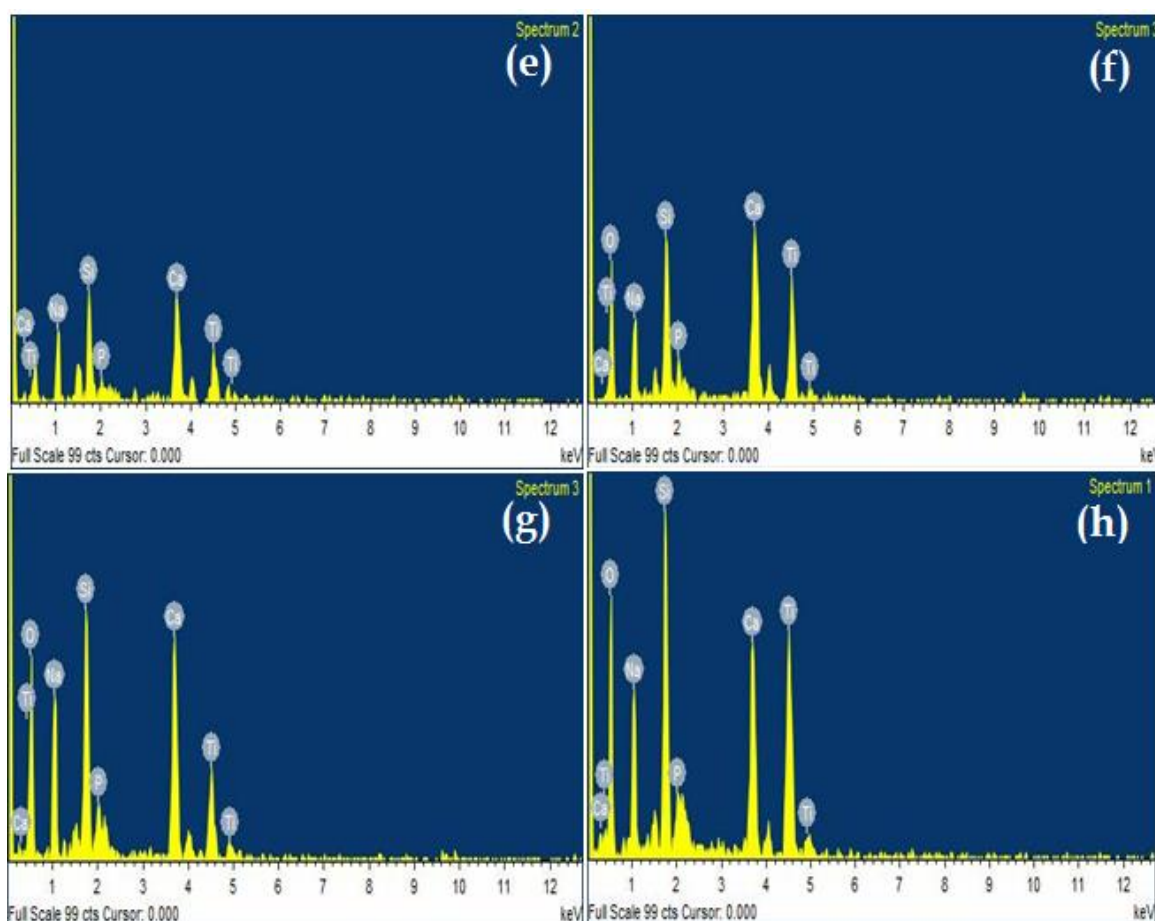


Figure 4.4 SEM (a-d) and EDAX (e-h) of the BG/HA/TiO<sub>2</sub> composites for BGHATi1, BGHATi2, BGHATi3 and BGHATi4 composites post-immersion in SBF.

#### 4.3.5 pH behaviour of biocomposite

The variation in pH values of simulated body fluid (SBF) after soaking of biocomposite for various time periods is shown in Fig.4.5. It was observed that the pH of all samples showed the similar tendency of behavior [Marta Cerrutia et al. 2005]. The maximum pH values were recorded on one day of immersion. The change of pH of SBF solution can be explained by ion exchange process on the glass surface. Cations such as Na<sup>+</sup> or Ca<sup>2+</sup> near the glass surface can go into solution in exchange for H<sup>+</sup> or H<sub>3</sub>O<sup>+</sup> ions from the solutions which result in pH increase after specific point and decrease in pH can be explained by considering the precipitation of calcium phosphates and carbonates. The

update of carbonate and phosphate ions shifts the equilibriums towards the products side, thus causing a decrease in the pH [Delia S. Brauer et al. 2010]. The sequence of reactions occurred in SBF after immersion of biocomposite for various time periods are in favor of the formation of hydroxyapatite layer on the surface of the samples [V.R. Mastelaro et al. 2000; P. Ducheyne et al. 1999].

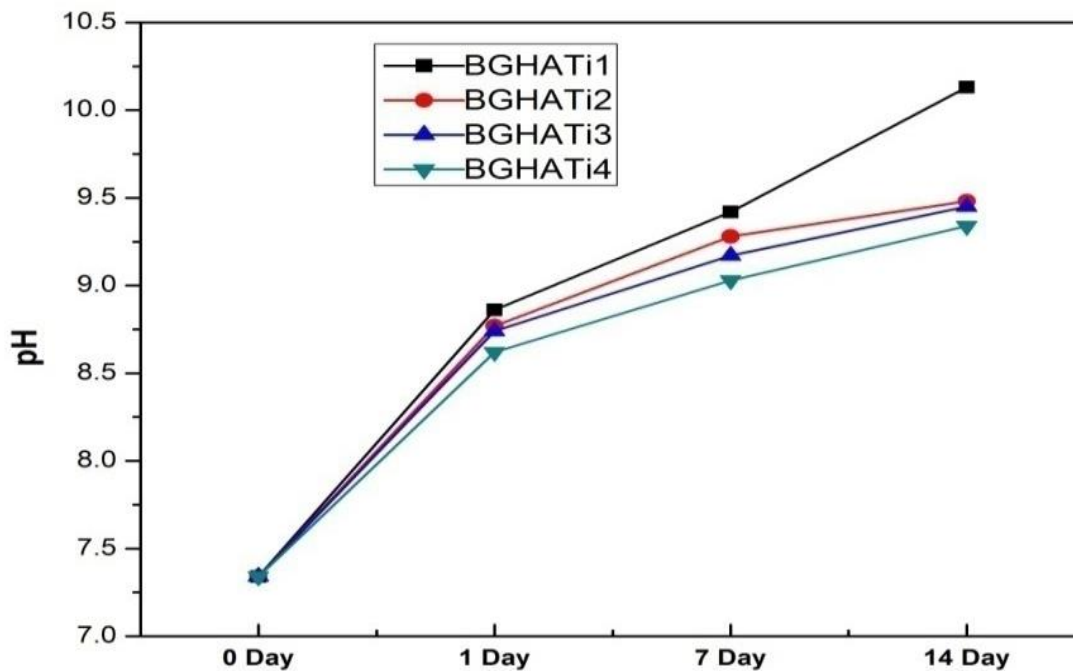
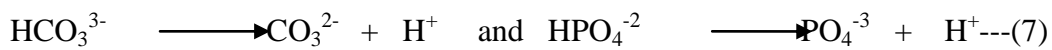


Figure 4.5 pH behaviour of biocomposite (BGHATi1, BGHATi2, BGHATi3, BGHATi4).

### 4.3.6. Density, Compressive Strength and Hardness of biocomposites

Table 4.2: Density ( $\rho$ ), longitudinal velocity ( $V_L$ ), transverse velocity ( $V_T$ ), young's modulus, shear modulus, bulk modulus and poisson's ratio of biocomposites.

Sample	Density ( $\rho$ ) ( $\text{gm/cm}^3$ )	$V_L$ (m/s)	$V_T$ (m/s)	Young's modulus E(GPa)	Shear modulus G(GPa)	Bulk modulus K(GPa)	Poisson's ratio ( $\nu$ )
BGHATi1	2.62	5489	3114	47	25	33	0.2627
BGHATi2	2.72	5605	3210	52	28	35	0.2559
BGHATi3	2.77	5716	3312	75	30	49	0.2472
BGHATi4	2.82	5886	3422	82	33	53	0.2447

The density increased rapidly when the pellet samples were sintered at 1150°C and 1250°C due to the partial HA decomposition into  $\alpha$ -TCP and TTCP. The density of biocomposite sintered at 1150°C increased with increasing HA and TiO<sub>2</sub> content as shown in Fig.6 because the density of titanium is more than 45S5 bioglass and HA.

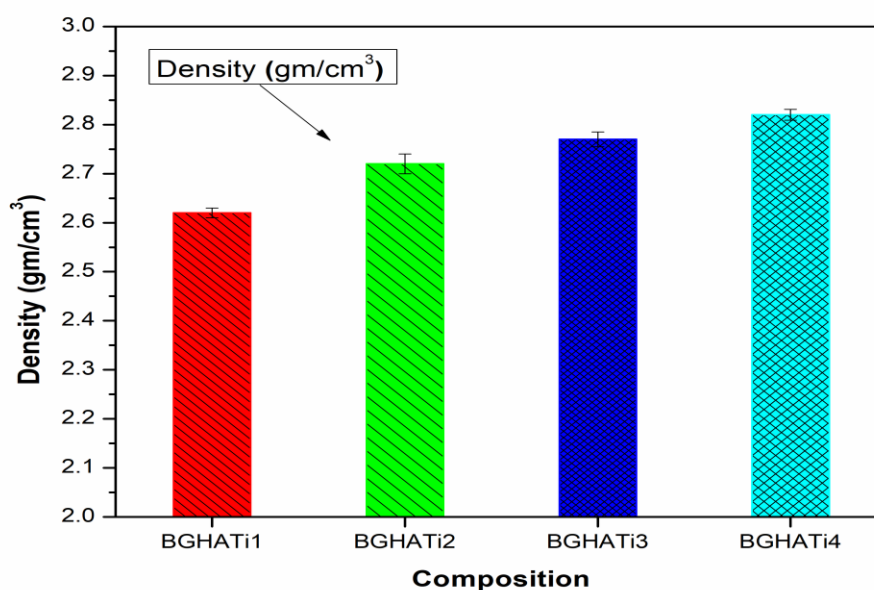


Figure 4.6 Variations of density in different HA and titania reinforced with bioglass composites.

Variation of compressive strength depending on reinforcement content and sintering temperature has shown in Fig.4.7. The figure shows that increasing reinforcement content from (5, 10, 15 and 20) wt.% increased the compressive strength from 41 to 104 MPa and hardness value from 125 to 377 for sintering at 1150°C. Such a phenomenon can be attributed to the occurrence of a new phase among bioglass, HA and TiO<sub>2</sub> for higher sintering temperatures.

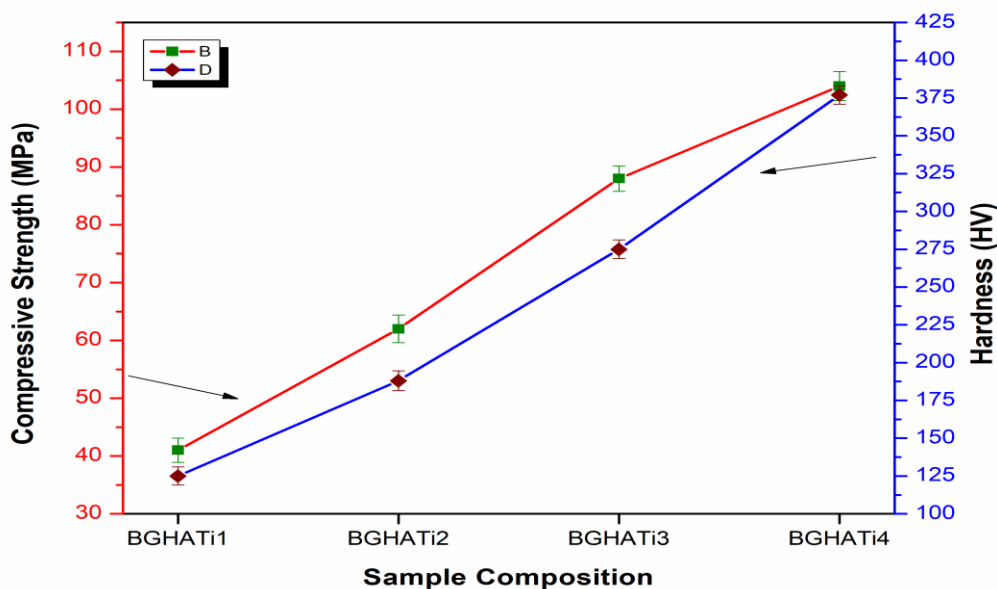
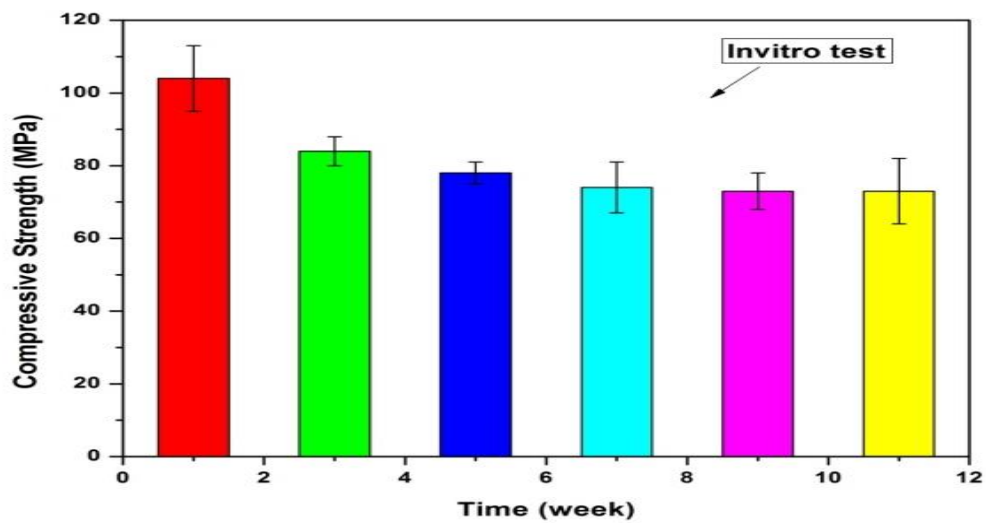


Figure 4.7 Variation of compressive strength and hardness depending on reinforcement content of pellet samples.

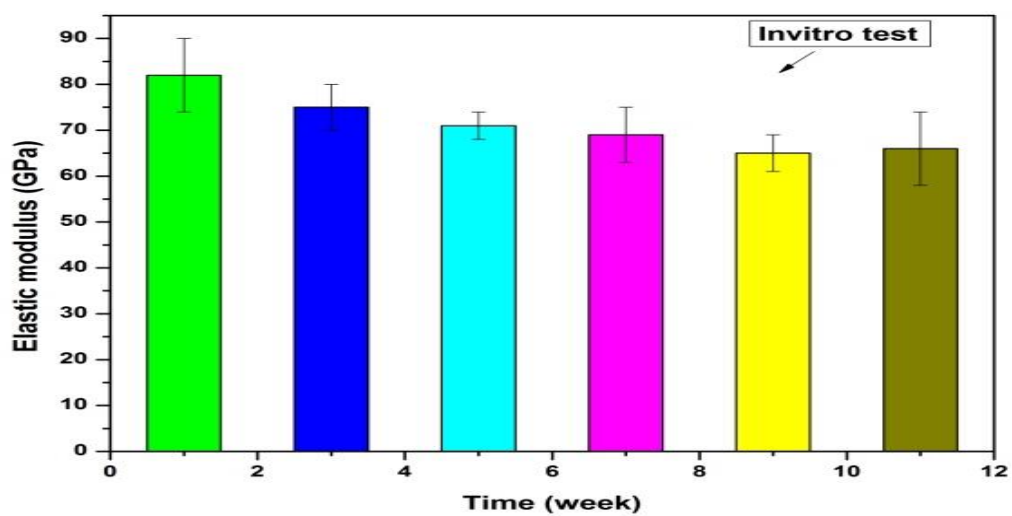
#### 4.3.7. Degradation of compressive strength of biocomposite during in vitro test

The compressive strength and elastic modulus of the scaffolds after immersion in SBF in vitro are shown in Fig.4.8(a) as a function of immersion time or implantation time. The strength and modulus decreased rapidly during the first three weeks but more slowly after that. This trend was independent of the in vitro environment. The strength decreased from the fabricated value of 104±8MPa to 84±5MPa after three weeks in

SBF in vitro test. After 12 weeks, the strength of the scaffolds immersed in SBF was  $73\pm 8$ MPa. The elastic modulus of the scaffolds decreased from the fabricated value of  $82\pm 8$ GPa to  $75\pm 5$ GPa after 3 weeks in SBF in vitro Fig.4.8(b). The modulus of the scaffolds was  $66\pm 8$ GPa, respectively after 12 weeks in SBF and in vitro environment.



(a)



(b)

Figure 4.8 (a) Compressive strength and (b) elastic modulus as a function of time for HA and TiO<sub>2</sub> reinforcement bioglass biocomposites after immersion in simulated body fluid (SBF) in vitro test.

#### 4.3.8. Elastic properties of HA and TiO<sub>2</sub> reinforcement of biocomposites

The results indicate that the elastic moduli showed an anomalous with an initial addition of HA, TiO<sub>2</sub> and it increases with the further addition of HA, TiO<sub>2</sub> content as shown in Fig.4.9. In BGHATi1 and BGHATi4 biocomposite, the measured Young's and shear moduli ranges respectively from 47 to 82 GPa and 25 to 33 GPa. Similarly, the young's and bulk moduli ranges from 47 to 82 GPa and 33 to 53 GPa Fig.4.9, 4.10 for BGHATi1 and BGHATi4 biocomposites. The increase in elastic moduli is due to an increase in the rigidity of bioglasses and TiO<sub>2</sub> content (A. V. Gayathri Devi et al.2006).

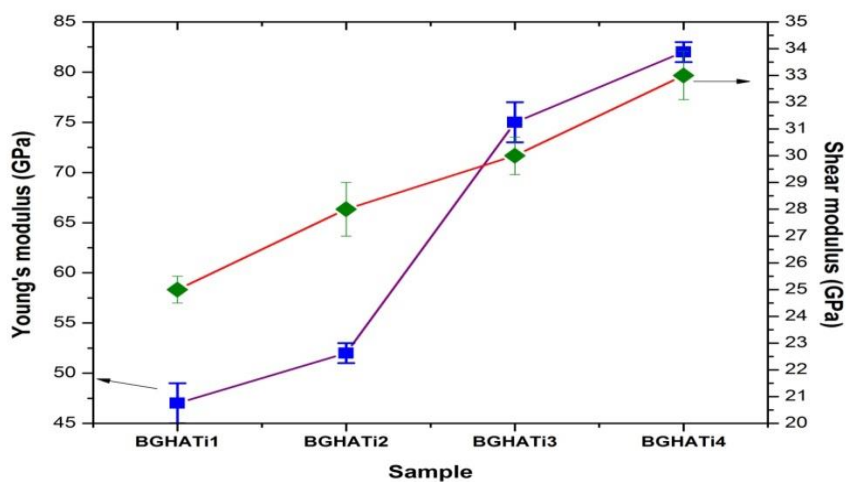


Figure 4.9 Young's modulus and shear modulus of biocomposites (BGHATi1, BGHATi2, BGHATi3, BGHATi4).



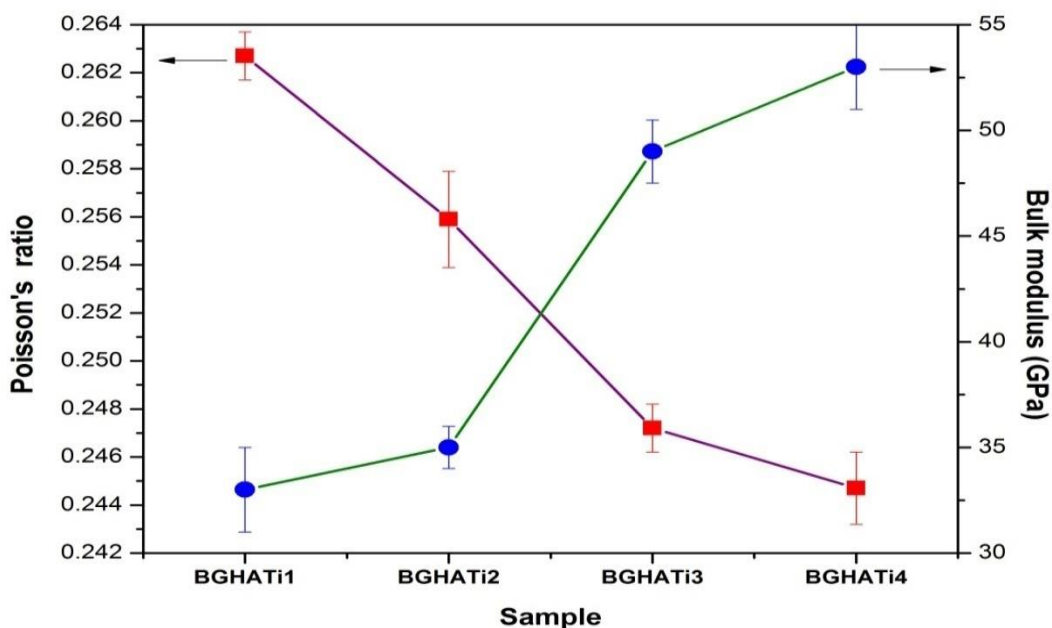


Figure 4.10 Bulk modulus and poisson's ratio of biocomposites (BGHATi1, BGHATi2, BGHATi3, BGHATi4).

#### 4.4. Conclusion

Biocomposites with the addition of HA and  $\text{TiO}_2$  in Bioactive glass (45S5) are prepared respectively using the sintering process. The presence of  $\text{TiO}_2$  in silicate-based 45S5 bioactive glass network results in higher rigidity which is explored from the observed increase in glass density. Due to the higher bonding ability of  $\text{TiO}_2$ , its results in an increase in ultrasonic velocity. The elastic constants results support the above observation. The thermal treatment of silicate-based glasses results in the release of stresses from the glass and the possible formation of crystalline phases along with the residual glassy phases.

$\text{Ti}^{2+}$  ion was introduced in the glass composition for  $\text{Si}^{4+}$  ion in different concentrations (0-20 wt%) to yield a non-charge valence series of bioglass based biocomposites. The increase of HA and  $\text{TiO}_2$  content in bioglass composites increase density, compressive strength, young's, shear and bulk modulus while the Poisson's ratio remained nearly

constant. The mechanical property of the samples can be measured without any destruction of the biocomposites since the biomaterials are very expensive to prepare.

\*\*\*